Including High-Frequency Surface Diffraction in a Hybrid FEBI-MLFMM-UTD Method

Manushanker Balasubramanian

Fraunhofer FHR, Germany

Alberto Toccafondi, Stefano Maci

Department of Information Engineering

University of Siena, Italy

Fraunhofer
FHR

Outline

- Motivations
- Introduction to FEBI-MLFMM-UTD method
- FEBI-MLFMM-UTD – Surface diffraction
- Ray Tracing on NURBS Surfaces
- Numerical examples
- Conclusion and outlook

Motivations

- Implementation of numerical methods for
  - Accurate prediction of field scattered by large objects
  - RCS prediction
  - Installed antenna performance

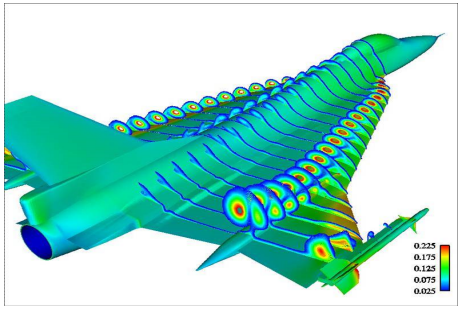

Fraunhofer
FHR

Introduction to FEBI-MLFMM-UTD method

- Finite Element Boundary Integral (FEBI) method is used for computing electromagnetic fields scattered by objects made up of PEC and dielectric materials
- CFIE for the Boundary integral method is

$$[Z_J^{CFIE}]\{H\} + [Z_M^{CFIE}]\{E\} = \{b\}$$

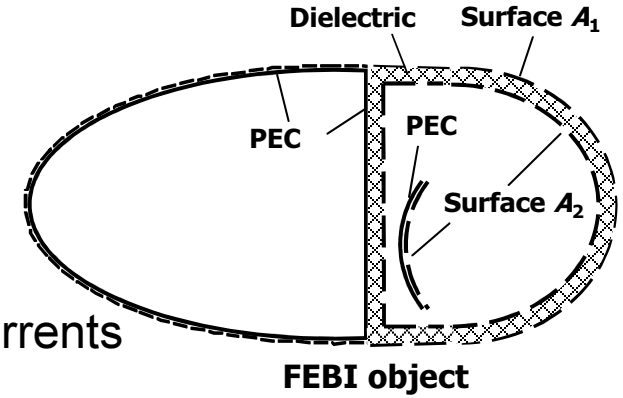

$\{H\}, \{E\}$ unknown electric and magnetic surface currents

$\{b\} \rightarrow$ excitation vector $[Z_{J,M}^{CFIE}] \rightarrow$ coupling matrices

- Coupling matrices are dense resulting in $O(N^2)$ computational complexity for performing matrix vector products, N is the number of unknowns

Introduction to FEBI-MLFMM-UTD method

- Fast Multipole Method (FMM) reduces the complexity from $O(N^2)$ to $O(N^{3/2})$
- Using multilevel version of FMM one further reduces the complexity to $O(N \log N)$
- Further computational gain can be achieved when evaluating the fields scattered by large objects using ray methods like
  - Uniform Theory of Diffraction (UTD)
  - Physical Theory of Diffraction (PTD)

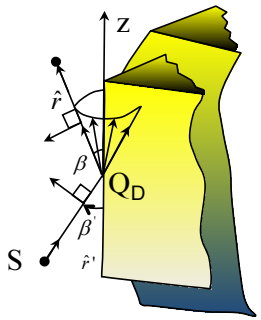

wedge diffraction

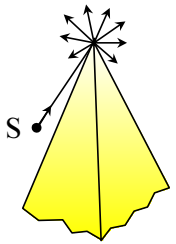

tip diffraction

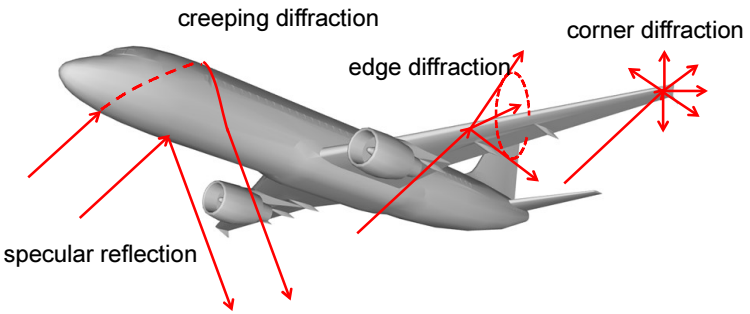

Introduction to FEBI-MLFMM-UTD method

- [1] introduces a method for coupling the fields scattered by a large planar object evaluated by using UTD into the Fast Multipole Method
- UTD reflected and wedge diffracted field contributions were only considered in the work of [1]
- In this work we propose a technique for including UTD surface diffracted fields that are scattered from a curved surface
- We use a Non-Uniform Rational B-splines (NURBS) representation for describing arbitrarily shaped surfaces
- Ray tracing pertinent to UTD is performed directly on NURBS surfaces

[1] A. Tzoulis, T.F. Eibert, "A Hybrid FEBI-MLFMM-UTD Method for Numerical Solutions of Electromagnetic Problems Including Arbitrarily Shaped and Electrically Large Objects", IEEE Trans. Antennas Propagat., vol 53, no. 10, pp. 3358-3366, October 2005.

FEBI-MLFMM-UTD – Surface diffraction

- UTD surface diffraction describes the behaviour of the electromagnetic waves that creeps along a curved surface
- Dyadic Green's function for the BI-UTD method can be represented as the sum of contributions in the absence of the object treated by UTD and that due to UTD field scattered by the object

$$\bar{\mathbf{G}}^{E}_{J,tot}(\mathbf{r}_m, \mathbf{r}_n) = \bar{\mathbf{G}}^{E}_{J}(\mathbf{r}_m, \mathbf{r}_n) + \bar{\mathbf{G}}^{E}_{J,UTD}(\mathbf{r}_m, \mathbf{r}_n)$$

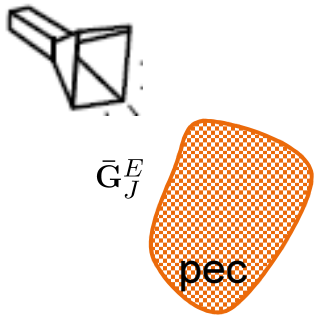

FEBI-MLFMM-UTD – Surface diffraction

- UTD surface diffraction describes the behaviour of the electromagnetic waves that creeps along a curved surface
- Dyadic Green's function for the BI-UTD method can be represented as the sum of contributions in the absence of the object treated by UTD and that due to UTD field scattered by the object

$$\bar{\mathbf{G}}^{E}_{J,tot}(\mathbf{r}_m, \mathbf{r}_n) = \bar{\mathbf{G}}^{E}_{J}(\mathbf{r}_m, \mathbf{r}_n) + \bar{\mathbf{G}}^{E}_{J,UTD}(\mathbf{r}_m, \mathbf{r}_n)$$

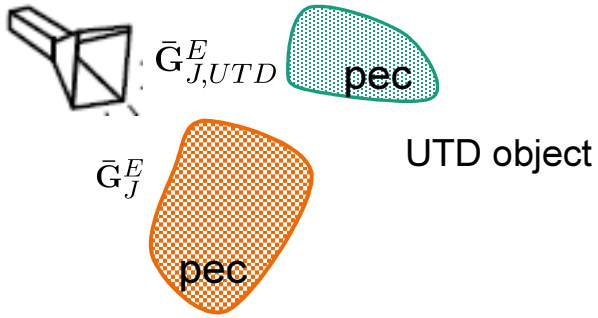

- $\bar{\mathbf{G}}^{E}_{J,UTD}(\mathbf{r}_m, \mathbf{r}_n)$ is assumed to be associated only with surface diffraction

FEBI-MLFMM-UTD – Surface diffraction

- The ray contribution to the Green's function may be represented as [Pathak 1980]

$$\bar{\mathbf{G}}^{E}_{J,UTD}(\mathbf{r}_m,\mathbf{r}_n) = \sum_l A^d_l(s^d_l)e^{-j\kappa s^d_l}e^{-j\kappa t_l}\underline{\underline{\tilde{T}}}_l\cdot\bar{\mathbf{G}}^{E}_{J}(\mathbf{r}_{Q'_l},\mathbf{r}_n)$$

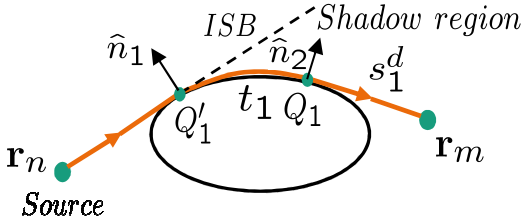

- Where l is the number of surface diffracted rays, t_l is the arc length of the corresponding geodesic path and $\underline{\underline{\tilde{T}}}_l$ is the dyadic surface diffraction coefficient
- $\underline{\underline{\tilde{T}}}_l$ is expressed as $\underline{\underline{\tilde{T}}}_l = \tilde{T}^s_l\hat{b}_1\hat{b}_2 + \tilde{T}^h_l\hat{n}_1\hat{n}_2$ which is given as

$$\tilde{T}^{s,h}_l = -\sqrt{m_l(Q'_l)m_l(Q_l)}\sqrt{\frac{2}{\kappa}}\cdot\left\{\frac{e^{-j\frac{\pi}{4}}}{2\xi^d_l\sqrt{\pi}}[1-F(X^d_l)]+\hat{P}^{s,h}(\xi^d_l)\right\}\sqrt{\frac{d\eta_{Q'_l}}{d\eta_{Q_l}}}$$

- $\tilde{T}^{s,h}_l$ are soft and hard dyadic coefficients
- $\sqrt{\frac{d\eta_{Q'_l}}{d\eta_{Q_l}}}$ describes the spreading of a ray tube on the curved surface

FEBI-MLFMM-UTD – Surface diffraction

- For including surface diffracted fields in FMM, the path vectors from the source current to the attachment point $\mathbf{r}_{Q_l'n}$ and from the detachment point to the test current $\mathbf{r}_{mQ_l}$ can be represented as

$$\mathbf{r}_{Q_l'n} = \mathbf{r}_{n'n} + \mathbf{r}_{Q_l'n'}$$
$$\mathbf{r}_{mQ_l} = \mathbf{r}_{mm'} + \mathbf{r}_{m'Q_l}$$

- When $|\mathbf{r}_{Q_l'n'}| \gg |\mathbf{r}_{n'n}| \& |\mathbf{r}_{m'Q_l}| \gg |\mathbf{r}_{mm'}|$

  by Taylor approximation

$$|\mathbf{r}_{Q_l'n}| = |\mathbf{r}_{Q_l'n'}| - \hat{\mathbf{r}}_{Q_l'n'} \cdot \mathbf{r}_{n'n}$$
$$|\mathbf{r}_{mQ_l}| = |\mathbf{r}_{m'Q_l}| - \hat{\mathbf{r}}_{m'Q_l} \cdot \mathbf{r}_{mm'}$$

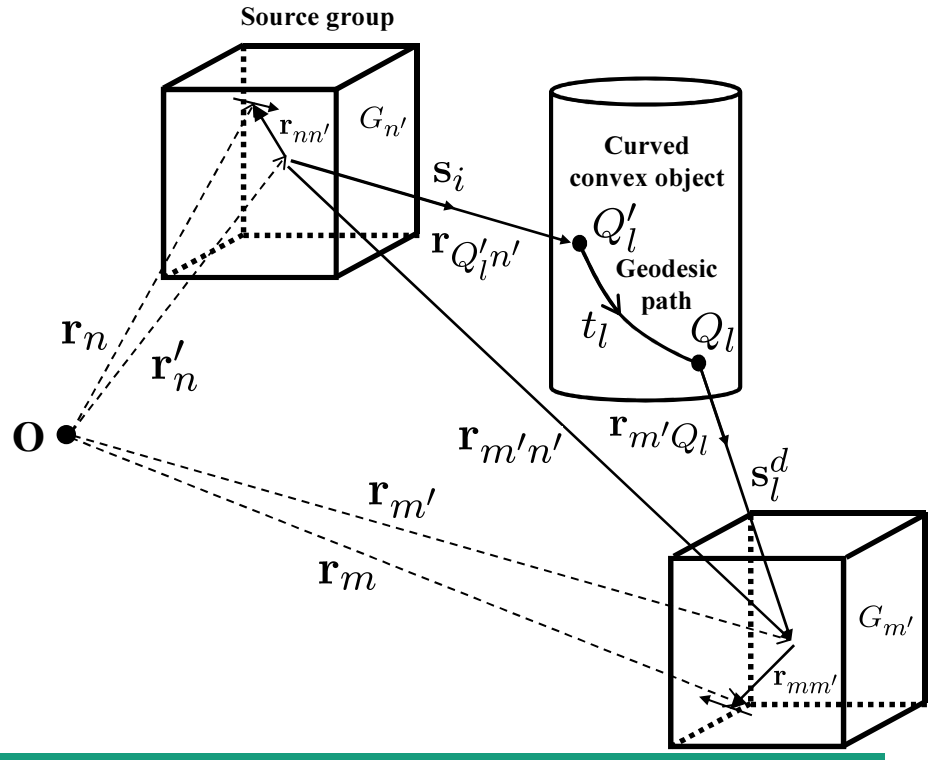

FEBI-MLFMM-UTD – Surface diffraction

- Using the far field approximation dyadic UTD Green's function is given as

$$\bar{\mathbf{G}}^{E}_{J,UTD}(\mathbf{r}_m,\mathbf{r}_n) = \sum_l e^{j\kappa(\hat{\mathbf{r}}_{m'Q_l}\cdot\mathbf{r}_{mm'})} A^d_l(s^d_l) e^{-j\kappa(r_{m'Q_l})} \cdot e^{-j\kappa t_l} \underline{\underline{\widetilde{T}}}_l T^{FF}_L(\kappa r_{Q'_l n'}) \cdot \left(-j\frac{\omega\mu}{4\pi}\right)\left(\underline{\underline{I}} - \hat{\mathbf{r}}_{Q'_l n'}\hat{\mathbf{r}}_{Q'_l n'}\right) e^{j\kappa(\hat{\mathbf{r}}_{Q'_l n'}\cdot\mathbf{r}_{n'n})}$$

- Where

$$T^{FF}_L(\kappa r_{Q'_l n'}) = \frac{e^{-j\kappa|\mathbf{r}_{Q'_l n'}|}}{|\mathbf{r}_{Q'_l n'}|}$$

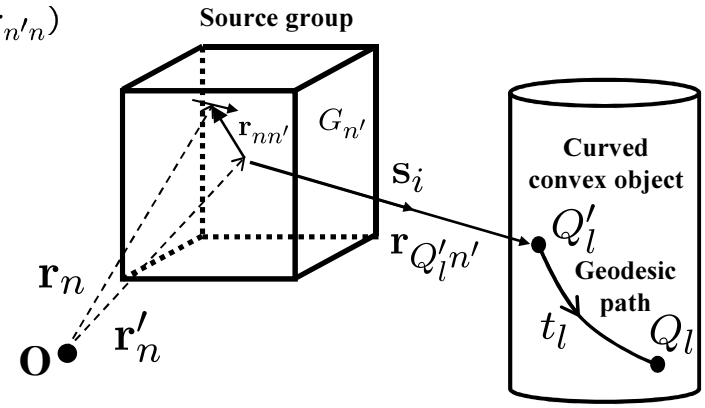

- Is the ray optical translation operator used for translating the fields from the centre of the source group to the attachment point Q'_l located on the surface

Ray Tracing on NURBS Surfaces

- In this work Non-Uniform Rational B-splines (NURBS) representation is used for describing curved surfaces
- For determining the surface diffracted fields from a object
  - Compute geodesic path
  - Locate Shadow Boundary Curves (SBC)
  - Evaluate the ray spreading factor $\sqrt{\frac{d\eta_{Q_1'}}{d\eta_{Q_1}}}$

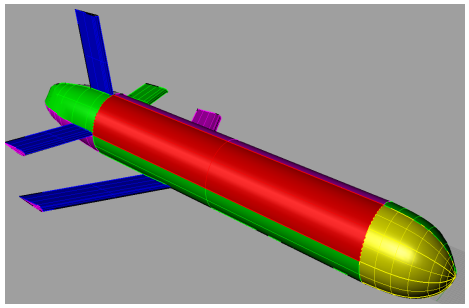

- Equation of a geodesic is solved as an initial value problem
- SBC are located by computing the silhouette curves
- Ray spreading factor is computed numerically

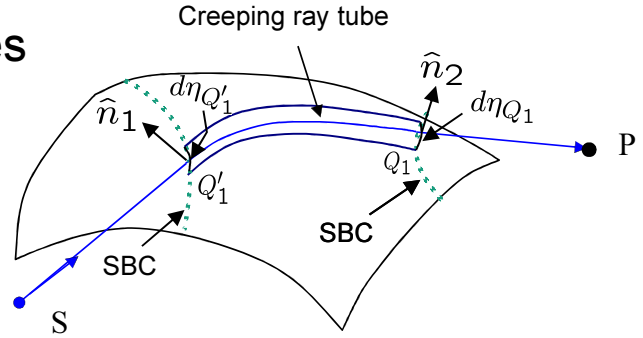

Ray Tracing on NURBS Surfaces

- For finding reflection points on a NURBS surface we use the Method of Successive Approximation (MSA) approach [3]
- This method requires few iterations for finding reflection point for a given observation point located in the lit regions of the given object
- But convergence problems were faced as the observation point approaches the incident shadow boundaries (ISB)
- In work we modified MSA algorithm by using Newton method for cases of observation points that approaches the ISB
- Routines are also implemented for classifying lit and shadow regions around a given surface

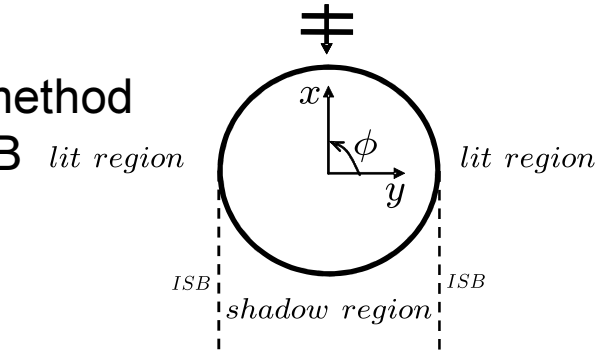

[3] Gordon, W.B., "Reflections From Multiple Surfaces Without Edges," Antennas and Propagation, IEEE Transactions on , vol.58, no.10, pp.3222,3230, Oct. 2010

Numerical examples

- A circular cylinder with spherical end caps is illuminated by a half wave length antenna oriented parallel to the axis of the cylinder and is located at 10λ from z axis
- Antenna is operating at frequency 10 GHz and fed by a voltage gap of amplitude 1 V/m
- Observation points are located at a distance $r = 50\lambda$ on the $\theta = \pi/2$ plane, for a spherical coordinate system placed at the centre of the cylinder

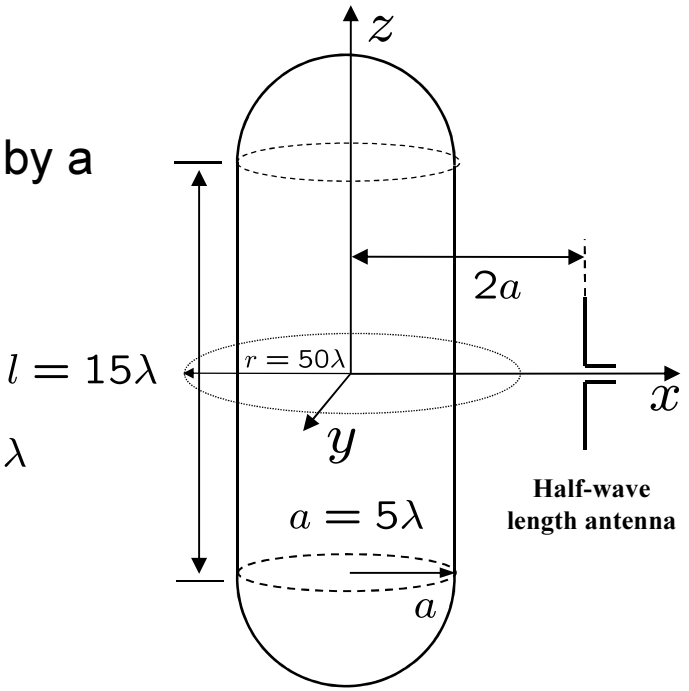

Numerical examples

- A circular cylinder with spherical end caps is illuminated by a half wave length antenna oriented parallel to the axis of the cylinder and is located at 10λ from z axis

- Antenna is operating at frequency 10 GHz and fed by a voltage gap of amplitude 1 V/m

- Observation points are located at a distance $r = 50\lambda$ on the $\theta = \pi/2$ plane, for a spherical coordinate system placed at the centre of the cylinder

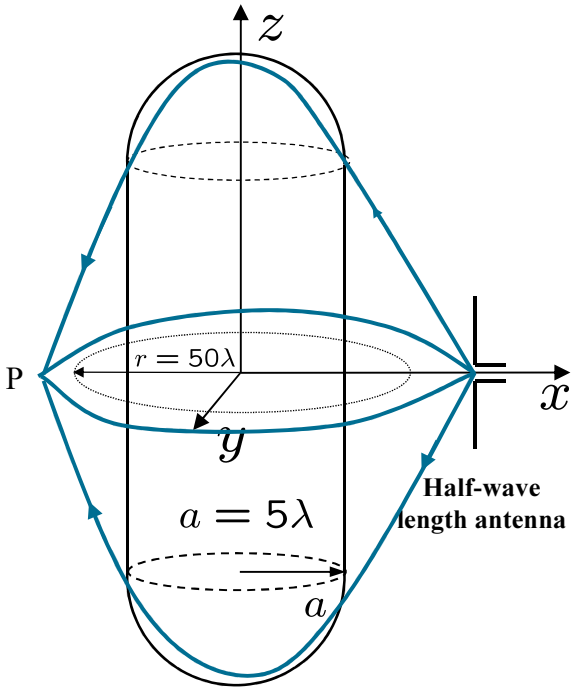

Numerical examples

- Number of unknowns
  - Reference MLFMM : 155564
  - FEBI-MLFMM-UTD: 11
- Computation time
  - Reference MLFMM : 2369 sec
  - FEBI-MLFMM-UTD: 900 sec
- Computed on the Intel(R) Core(TM) i7-3960X CPU @ 3.30GHz computer
- Discrepancies at $\phi \approx 0°$ difference due to modelling of antenna in reference and FEBI-MLFMM-UTD
- Reference antenna (wire segments) and FEBI-MLFMM-UTD antenna (meshed surface)

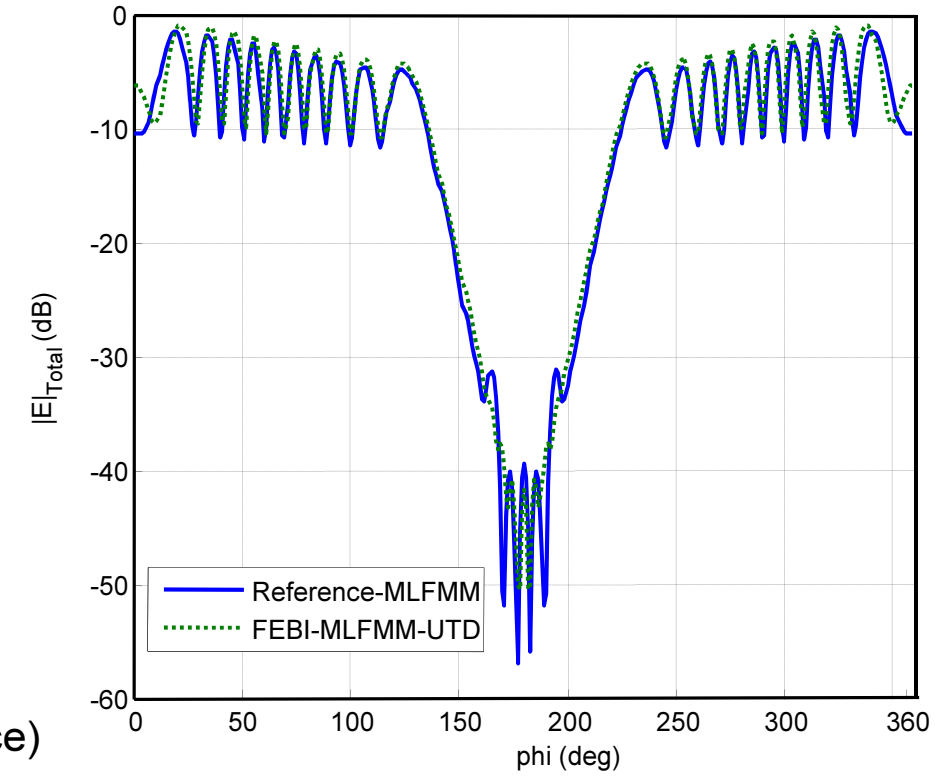

Fraunhofer FHR

Numerical examples

- A metallic airfoil is illuminated by the same half wave length antenna of the previous example operating at $f = 10$ GHz and fed by voltage gap of amplitude 1 V/m
- Rectangular coordinate system is considered to be located on the leading edge of the airfoil with its z-axis parallel to the trailing edge
- The half-wave dipole axis is parallel to the z-axis and located at a distance of $h = 6\lambda$ from the xz- plane
- Observation points are located at a distance $r = 50\lambda$ on the $\theta = \pi/2$ plane, for a spherical coordinate system placed at the leading edge of airfoil

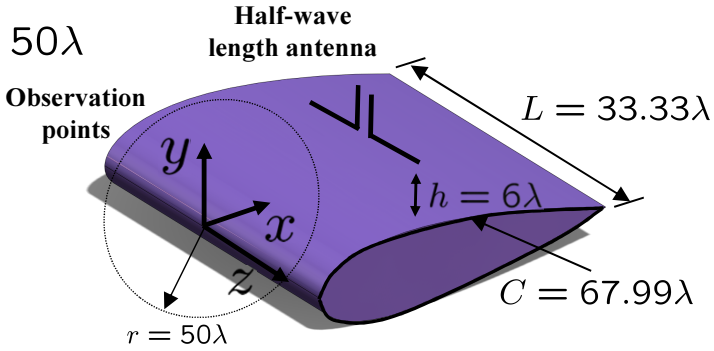

Numerical examples

- A metallic airfoil is illuminated by the same half wave length antenna of the previous example operating at $f = 10$ GHz and fed by voltage gap of amplitude 1 V/m
- Rectangular coordinate system is considered to be located on the leading edge of the airfoil with its z-axis parallel to the trailing edge
- The half-wave dipole axis is parallel to the z-axis and located at a distance of $h = 6\lambda$ from the xz- plane
- Observation points are located at a distance $r = 50\lambda$ on the $\theta = \pi/2$ plane, for a spherical coordinate system placed at the leading edge of airfoil

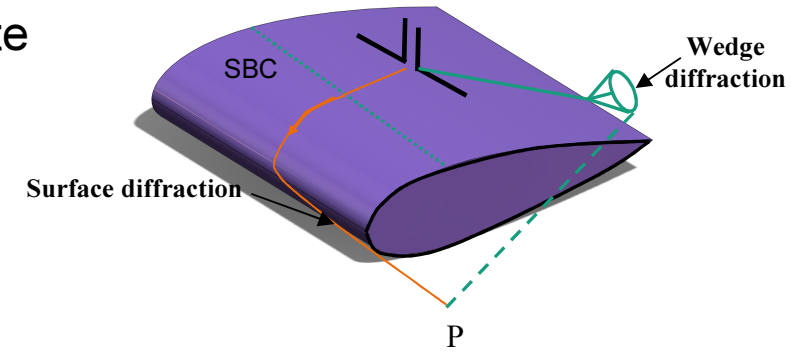

Numerical examples

- Number of unknowns
  - Reference MLFMM : 497838
  - FEBI-MLFMM-UTD: 11
- Computation time
  - Reference MLFMM : 2342 sec
  - FEBI-MLFMM-UTD: 1500 sec
- Computed on the Intel(R) Core(TM) i7-3960X CPU @ 3.30GHz computer
- Discrepancies at $\phi \approx 260^{\circ}$ deep shadow region

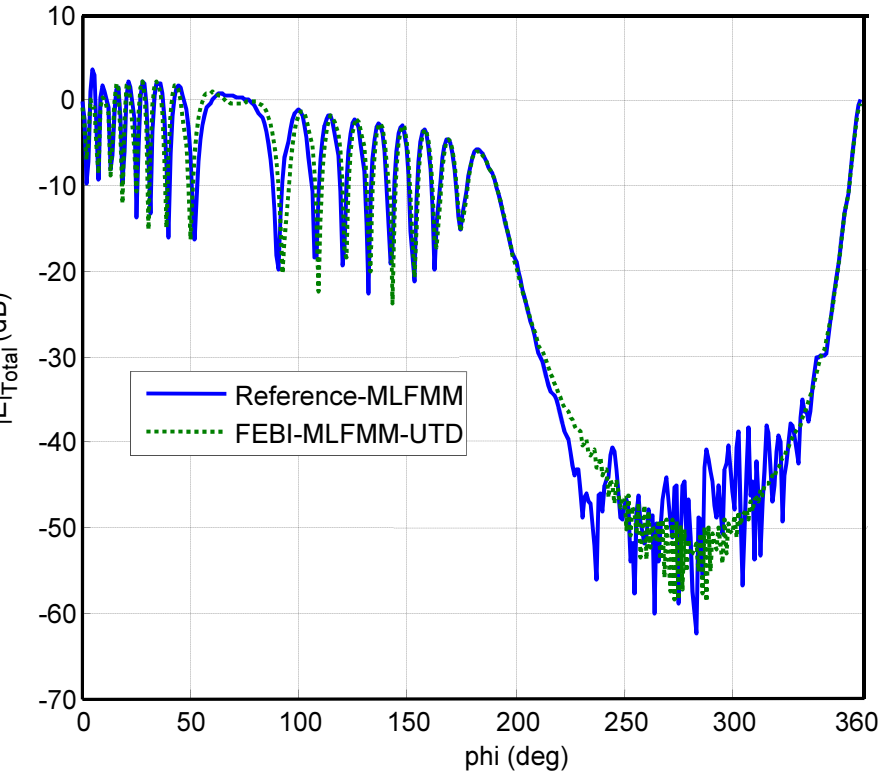

Fraunhofer FHR

Numerical examples – Interpretation in terms of UTD

- Forward scattering region corresponds to the deep shadow region
- Contains contributions only from the UTD surface and wedge diffracted fields which are excited at the leading and trailing edges of the airfoil
- Variation of the total field in this region can be described as interference between these two dominant contributions and the result obtained by our approach matches quite well to this statement
- The random oscillatory behaviour in the reference curve might be due to higher order wedge diffraction
- From lateral faces of the airfoil that are not yet included in the FEBI-MLFMM-UTD approach

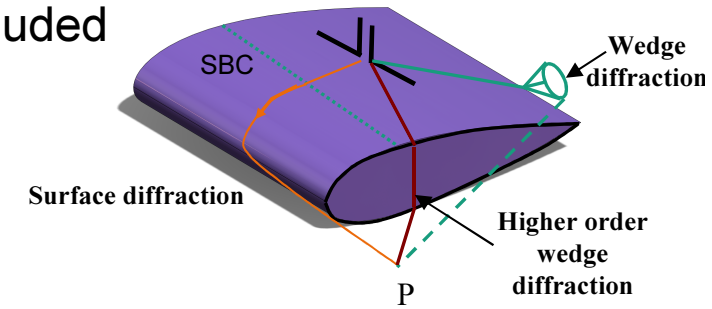

Numerical examples

- A metallic NASA almond is illuminated by the same half wave length antenna as in previous examples
- Coordinate system is located at the rounded end of the almond and almond is oriented parallel to z-axis
- The antenna axis is parallel to the z-axis and located at a distance of $h = 20\lambda$ from the xz- plane
- Observation points are located on a azimuthal plane at a distance $r = 10\lambda$

$xy-$ azimuthal plane

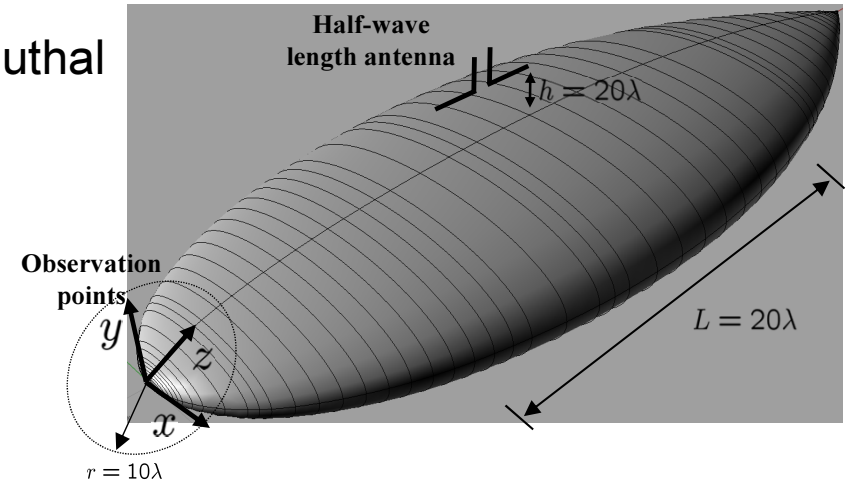

Numerical examples

- A metallic NASA almond is illuminated by the same half wave length antenna as in previous examples
- Coordinate system is located at the rounded end of the almond and almond is oriented parallel to z-axis
- The antenna axis is parallel to the z-axis and located at a distance of $h = 20\lambda$ from the xz- plane
- Observation points are located on a azimuthal plane at a distance $r = 10\lambda$

$xy-$ azimuthal plane

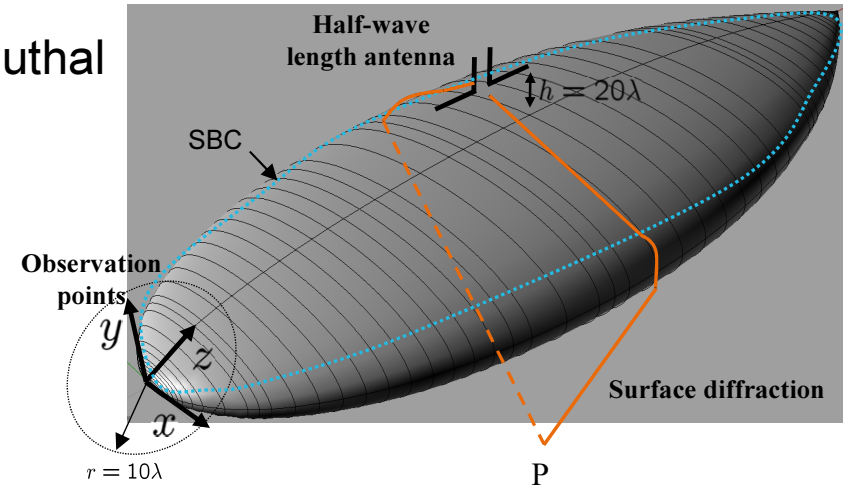

Numerical examples

- Number of unknowns
  - Reference MLFMM : 76143
  - FEBI-MLFMM-UTD: 11
- Computation time
  - Reference MLFMM : 2197 sec
  - FEBI-MLFMM-UTD:1050 sec
- Computed on the Intel(R) Core(TM) i7-3960X CPU @ 3.30GHz computer

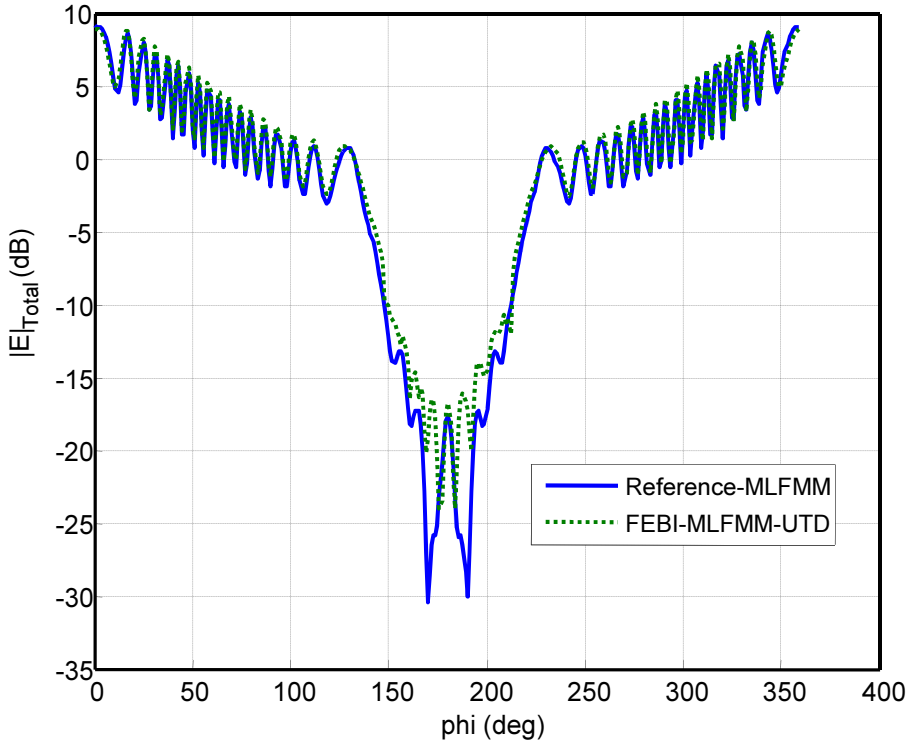

Fraunhofer FHR

Conclusion

- A new formulation for including surface diffracted fields into BI-FMM method is introduced
- Overview of the ray tracer that has been implemented is provided
- Numerical examples validating the effectiveness of the proposed approach is described

Future work:

- Computation of fields scattered by objects when illuminated by non elementary radiators
- Implementation of routines for calculating higher order wedge diffraction contributions by using UTD
- Ray tracing trimmed NURBS surfaces for handling more complex objects